



HAL
open science

Magnetic anisotropy modified by electric field in V/Fe/MgO(001)/Fe epitaxial magnetic tunnel junction

A. Rajanikanth, Thomas Hauet, François Montaigne, Stéphane Mangin,
Stéphane Andrieu

► **To cite this version:**

A. Rajanikanth, Thomas Hauet, François Montaigne, Stéphane Mangin, Stéphane Andrieu. Magnetic anisotropy modified by electric field in V/Fe/MgO(001)/Fe epitaxial magnetic tunnel junction. Applied Physics Letters, 2013, 103 (6), pp.062402. 10.1063/1.4817268 . hal-01276619

HAL Id: hal-01276619

<https://hal.science/hal-01276619v1>

Submitted on 13 Jul 2016

HAL is a multi-disciplinary open access archive for the deposit and dissemination of scientific research documents, whether they are published or not. The documents may come from teaching and research institutions in France or abroad, or from public or private research centers.

L'archive ouverte pluridisciplinaire **HAL**, est destinée au dépôt et à la diffusion de documents scientifiques de niveau recherche, publiés ou non, émanant des établissements d'enseignement et de recherche français ou étrangers, des laboratoires publics ou privés.

Magnetic anisotropy modified by electric field in V/Fe/MgO(001)/Fe epitaxial magnetic tunnel junction

A. Rajanikanth, T. Hauet, F. Montaigne, S. Mangin, and S. Andrieu

Citation: *Appl. Phys. Lett.* **103**, 062402 (2013); doi: 10.1063/1.4817268

View online: <http://dx.doi.org/10.1063/1.4817268>

View Table of Contents: <http://apl.aip.org/resource/1/APPLAB/v103/i6>

Published by the AIP Publishing LLC.

Additional information on *Appl. Phys. Lett.*

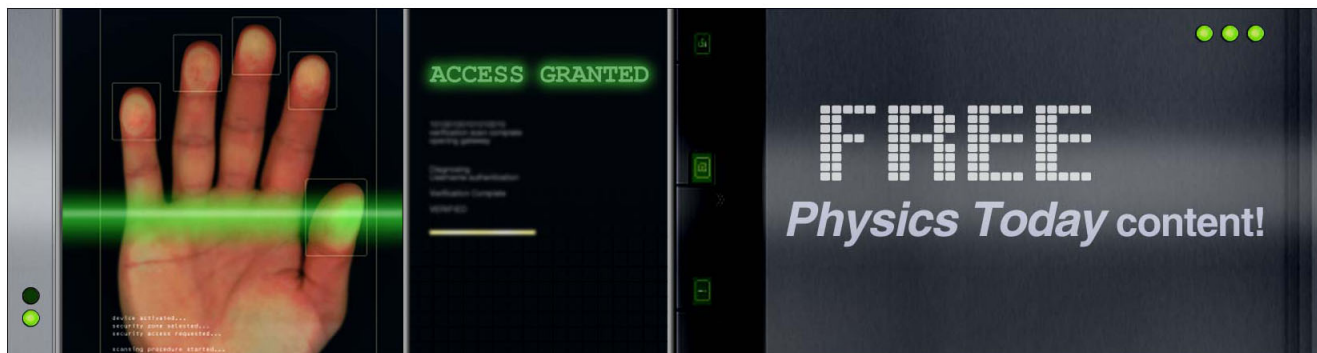
Journal Homepage: <http://apl.aip.org/>

Journal Information: http://apl.aip.org/about/about_the_journal

Top downloads: http://apl.aip.org/features/most_downloaded

Information for Authors: <http://apl.aip.org/authors>

ADVERTISEMENT



Magnetic anisotropy modified by electric field in V/Fe/MgO(001)/Fe epitaxial magnetic tunnel junction

A. Rajanikanth, T. Hauet, F. Montaigne, S. Mangin, and S. Andrieu^{a)}

Institut Jean Lamour, UMR CNRS 7198, Université de Lorraine, 54506 Vandoeuvre lès Nancy, France

(Received 22 April 2013; accepted 16 July 2013; published online 5 August 2013)

Single-crystalline V/Fe(0.7 nm)/MgO(1.2 nm)/Fe(20 nm) magnetic tunnel junctions are studied to quantify the influence of an electric field on the Fe/MgO interface magnetic anisotropy. The thinnest Fe soft layer has a perpendicular magnetic anisotropy (PMA), whereas the thickest Fe layer acts as sensor for magnetic anisotropy changes. When electrons are added at the PMA Fe/MgO interface (negative voltage), no anisotropy changes are observed. For positive voltage, the anisotropy constant decreases with increasing bias voltage. A huge $1150 \text{ fJ V}^{-1} \text{ m}^{-1}$ anisotropy variation with field is observed and the magnetization is found to turn from out-of-plane to in-plane of the sample with the applied voltage. © 2013 AIP Publishing LLC. [<http://dx.doi.org/10.1063/1.4817268>]

High density non-volatile memory is currently being developed to provide fast access and low energy consumption for the next generation of computers. Magnetic Random Access Memory (MRAM) is a promising candidate for these future devices. Major research efforts for MRAM focus on switching Magnetic Tunnel Junctions (MTJ) through spin transfer torque (STT)^{1,2} to create the next generation of MRAM, known as STT-MRAM. In these devices, a strong Perpendicular Magnetic Anisotropy (PMA) provides thermal stability³ but further reduction of the current density, J_c is still required for practical applications.

A promising route is to use electric-field induced switching which can be combined with electric-current switching. Recently, there have been several reports of electric field control of magnetic properties, such as magnetic anisotropy in piezoelectric/ferromagnetic bilayers^{4,5} or Curie temperature in ferromagnetic semiconductors.^{6,7} Unfortunately, most of these effects were observed at low temperatures due to low Curie temperature materials. Electric field induced magnetic property modification has recently been achieved in 3d transition metals like Fe, Ni, Co, or associated alloys with both high T_c and high magnetization, by biasing a dielectric in contact with a magnetic layer. This was first demonstrated on FePd⁸ and afterwards in Fe,⁹ showing an anisotropy modification through applied electric field in the dielectric. Recently tuning of the Curie temperature in Co films with electric fields has also been demonstrated.^{10,11} MTJ were used to detect the magnetic anisotropy change by measuring the resistance versus field response for different biases applied to the junction.¹² Theoretical studies of metallic systems have recently addressed this problem,^{13–16} explaining the effect by electrons accumulation or depletion at the magnetic metal/dielectric interface. Most of the reported experimental works were performed on FePt,⁸ Fe,^{9,18} FePd,^{8,17} CoFe,^{12,19} and CoFeB MTJs.^{20,21} In this work, the strong PMA observed on thin Fe layers epitaxially grown on bcc V(001) and covered by MgO²² is used to test the electric field effect on magnetic anisotropy. This structure is integrated as a free layer in a magnetic tunnel junction device to

probe its magnetic response to various electric fields through MgO barrier and to a magnetic field applied either in plane (IP) or perpendicular to the film plane.¹² The Fe PMA variation with bias voltage is thus extracted from Tunnel Magneto-Resistance (TMR).

Epitaxy of V(5 nm)/Fe(0.7 nm)/MgO(1.2 nm) was performed by molecular beam epitaxy (MBE), with a base pressure lower than 10^{-10} Torr, on MgO (001) single-crystals. Vanadium was deposited at room temperature (RT) and post-annealed at 600 °C. Fe was added at RT and annealed at a lower temperature of 400 °C to smooth the Fe surface, but avoid Fe/V intermixing observed in other samples annealed above 600 °C. The MgO barrier and hard magnetic Fe/Co top layer were then deposited at RT and not annealed. The final stacking used in this study is thus MgO(substrate)/V(10 nm)/Fe(0.7 nm)/MgO(1.2 nm)/Fe(5 nm)/Co(5 nm)/Au(5 nm). The epitaxial relationship, growth mode, number of deposited monolayers (ML), and surface flatness were controlled *in-situ* using reflection high energy electron diffraction (RHEED). The magnetic characterizations were performed at 300 K on full films using a commercial SQUID-VSM. UV lithography was used to pattern MTJ devices with a junction size of $30 \times 30 \mu\text{m}^2$. Typical TMR ratios between 1% and 5% were obtained depending on the magnetization configuration. These values are low compared with TMR results we have reported for MgO barriers—50% for 6 monolayers MgO and 200% for 12 monolayers MgO, but these differences cannot be ascribed to pinholes. The presence of pinholes in our process is statistically rare, and a similar electric behavior is observed on nearly all of the patterned MTJs. Such small TMR values may come from the fact that thin soft Fe layers are needed to get PMA and that a thin MgO barrier is required in order to limit the applied bias. The barrier resistance for such MgO thicknesses is not much larger than contact resistances but also contributes to limit the TMR values. In order to explore the magnetic configuration of the soft layer (SL) with bias voltage and applied magnetic field, magneto-resistance was measured applying H in the plane (H_{\parallel}) of the sample and along Fe(100), or out of the plane (H_{\perp}) of the sample. An Anisotropic Magneto-Resistance (AMR) effect cannot be excluded since the injected current is parallel or perpendicular to the magnetization depending on the applied field direction. We thus

^{a)} Author to whom correspondence should be addressed. Electronic mail: stephane.andrieu@univ-lorraine.fr

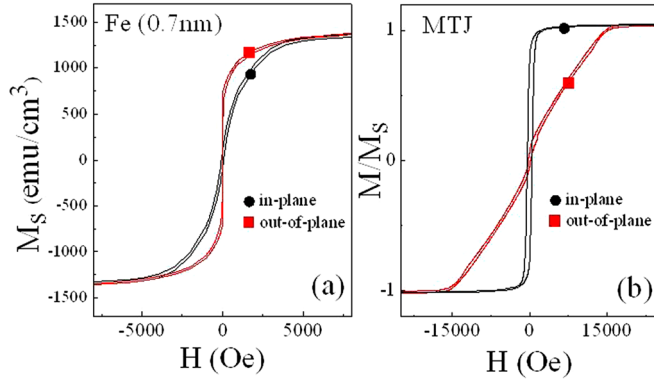


FIG. 1. (a) Magnetization vs field measurement of the V/Fe/MgO soft layer alone for both in-plane and out-of-plane applied magnetic field. (b) Similar measurement for the whole stacking, including the top Fe/Co hard layer.

report the resistance variation with applied field that includes both TMR and possible AMR effects.

The magnetic configuration of both soft and hard layers (HL) was first checked using hysteresis loop measurements by applying the magnetic field in and out of the sample plane (Fig. 1). The soft layer was first measured without the hard layer (Fig. 1(a)) which results in the magnetization being out-of-plane (OOP). By measuring the area between the IP and OOP loop in one quadrant, we extracted the effective magnetic anisotropy energy as follows:

$$K_{eff} = K_V + K_{shape} + \frac{K_s}{(t - t_{DL})} = \frac{1}{2} \mu_0 H_K \frac{M_s}{S(t - t_{DL})}, \quad (1)$$

where K_V is the bulk magnetic anisotropy, K_s the total interface anisotropy (V/Fe and Fe/MgO), K_{shape} the shape anisotropy, M_s the total sample moment (in emu), S the sample surface, t the thickness of the soft magnetic layer, and t_{DL} the thickness of dead magnetic layers (2ML in this system, see Ref. 22). As discussed in Ref. 22, this PMA originates from the Fe/MgO(001) interface ($K_v \ll K_s/t$), one thus get an effective Fe/MgO interface anisotropy per surface area that we note K_s^{eff} as follows:

$$K_s^{eff} = K_{shape}(t - t_{DL}) + K_s = \frac{1}{2} \mu_0 H_K \frac{M_s}{S}. \quad (2)$$

This experimental determination of K_s^{eff} by measuring H_K , M_s (in emu), and S does not depend on the Fe thickness, and so on the presence of dead layers. Consequently, measuring the variation of K_s^{eff} with the voltage gives the variation of K_s with the voltage, assuming that $K_{shape}(t - t_{DL})$ is not dependent on it. From Fig. 1(a), we extract $K_s^{eff} = 0.08$ erg/cm², i.e., 80 μ J/m², with an anisotropy field around 3 kOe. Fig. 1(b) shows magnetization versus field measured on a full film of the MTJ stacking. Since the top layer is much thicker than the bottom one, the signal mostly comes from Fe(5 nm)/Co(5 nm). The saturation magnetization for the hard layer is of the order of 1500 emu/cm³ and the anisotropy field is about 16 kOe. The demagnetization energy clearly favors an in-plane orientation of the HL magnetization at zero external field.

Figure 2 shows $\Delta R_V(H_{//})$ resistance variation as a function of the in-plane applied magnetic field for different bias voltage ΔV . Here, ($\Delta R = R(H) - R(H_{max})$) and $\Delta V = V_b - V_t$, where V_b is the voltage applied on the bottom V/Fe soft layer

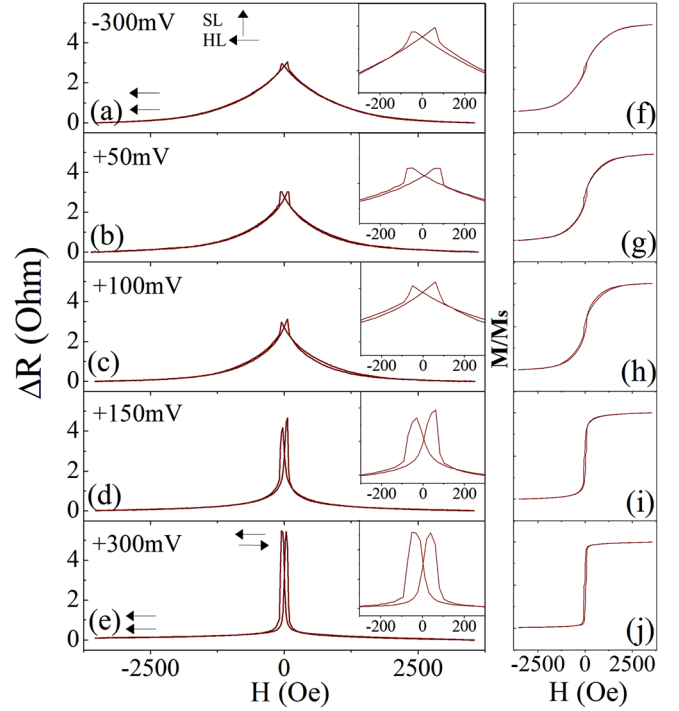


FIG. 2. $\Delta R_V(H_{//})$ measured at $\Delta V = -300$ (a), +50 (b), +100 (c), +150 (d), and +300 mV (e). $R(H_{//})$ zooms for low field range are shown in inset. The top and bottom arrows represent a schematic view of the magnetization orientation of the SL and HL, respectively. (f)–(j) are hysteresis loops of the soft layer for in-plane field deduced from $R(H_{//})$ curves using Eq. (3).

and V_t the voltage applied on the top Fe/Co hard layer. ΔV varied from -300 mV to $+300$ mV. It should be noted that when applying the bias, while the magnetic anisotropy is set faster than the experiment time resolution, the MTJ resistance was observed to vary for a period from few minutes to as much as 1 h (depending on the bias voltage amplitude) before reaching steady state. This behavior is observed on all the patterned MTJs and is reversible. The $\Delta R_V(H)$ measurements were thus performed after such a delay. This behavior is discussed at the end of the paper. For negative bias up to $+100$ mV (Figs. 2(a)–2(c)), the $\Delta R_V(H_{//})$ curves are similar and reflect the soft layer magnetization coherent rotation from OOP at zero magnetic field to IP (along the field direction) as the magnetic field amplitude increases. The measured saturation field around 3 kOe is close to the value extracted from Fig. 1(a). For bias higher than $+100$ mV, the $\Delta R_V(H_{//})$ curve's shape changes dramatically (Figs. 2(d) and 2(e)). Much sharper resistance transitions are observed. Such resistance loops are typical for MTJs where both electrodes show in-plane anisotropy. Therefore, we can conclude that the $+300$ mV bias has switched the soft Fe(0.7 nm) electrode anisotropy from OOP to IP. To further extract anisotropy field as a function of voltage, we calculated from the resistance data the ratio M_{ip}/M_s of the MTJ, with M_{ip} being the in-plane component of Fe(0.7 nm) magnetization. We used Eq. (3) as previously reported in Ref. 12:

$$\frac{M_{ip}}{M_s} = \frac{R_p}{R} \left(\frac{R_{\downarrow} - R}{R_{\downarrow} - R_p} \right), \quad (3)$$

where R_p is the parallel resistance at the saturation field and R_{\downarrow} is the resistance at zero field. Figures 2(f)–2(j) show the

extracted $M_{ip}(H)$ loops for the different biases. The loops are typical of hard axis loop for bias varying from -300 mV to $+100$ mV, meaning that the easy axis is out of plane. For bias higher than 100 mV (Figs. 2(i) and 2(j)), the $M_{ip}(H)$ loops are more typical of easy axis loop. The soft layer easy axis is thus in-plane.

Before analyzing similar $\Delta R_V(H)$ curves with the magnetic field perpendicular to the film plane, it must first be ensured that the ΔR is not coming from an AMR contribution. For that purpose, the resistance was recorded at $\Delta V = -300$ mV (OOP soft layer magnetization at $H = 0$) for both $H_{//}$ and H_{\perp} (Fig. 3). H was tuned up to 20 kOe since the anisotropy field of the hard layer is around 15 kOe (Fig. 1(b)). The MR results are consistent with magnetization measurements of Fig. 1. $R(H_{//})$ saturates above 3 kOe corresponding to the anisotropy field of the soft layer ($H_k(SL)$ in Fig. 3) while $R(H_{\perp})$ saturates around 16 kOe, the hard layer anisotropy field ($H_k(HL)$ in Fig. 3). At large fields for both $H_{//}$ and H_{\perp} , resistance values are the same meaning that AMR is negligible and that the main effect is TMR.

The field is then applied perpendicular (H_{\perp}) and the bias voltage is varied from -300 to $+300$ mV (Fig. 4). Again two kinds of $\Delta R_V(H_{\perp})$ curves are observed. For bias from -300 mV to $+50$ mV, the $\Delta R_V(H_{\perp})$ variation may be simply explained: the soft layer shows PMA and its magnetization remains perpendicular since H is applied out-of-plane. The hard Fe/Co layer has in-plane anisotropy and therefore rotates from OOP to IP when decreasing H_{\perp} . As a consequence, when the field decreases from 5 kOe to zero field, the angle between the hard and soft layer magnetization increases, leading to an increasing resistance. For voltages higher than 100 mV, both soft and hard layers tend to turn back along their in-plane easy axis. The hard layer starts rotating at 16 kOe, its anisotropy field, whereas the soft layer stays parallel to the field as long as its own anisotropy field is not reached. Between these two anisotropy fields, the resistance increases because the relative angle between the two magnetizations increases. Below the soft layer anisotropy field, the rotation of the soft layer decreases, leading to a decrease in the angle between magnetizations. Therefore, the field (marked with a star in Fig. 4) at which the resistance starts to decrease corresponds to the anisotropy field of the soft layer.

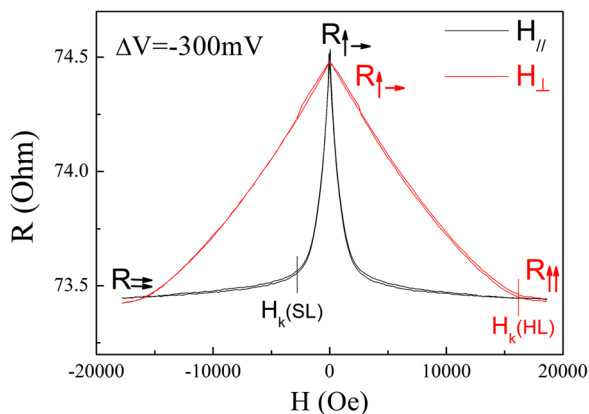


FIG. 3. $R(H)$ curves measured applying the magnetic field in-plane ($H_{//}$) and out-of-plane (H_{\perp}) at $\Delta V = -300$ mV. The resistance is the same at $H = 20$ kOe for both $H_{//}$ and H_{\perp} meaning that AMR is negligible.

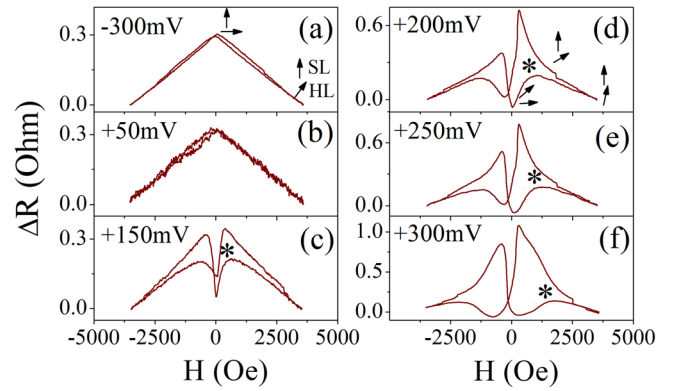


FIG. 4. $R_V(H_{\perp})$ curves measured applying the magnetic field out-of-plane for biases equal to (a) -300 mV, (b) $+50$ mV, (c) $+150$, (d) $+200$ mV, (e) $+250$ mV, and (f) $+300$ mV. The stars on the (c)-(f) give an estimation of the anisotropy field of the soft layer.

We can now quantify the influence of the bias on the soft layer anisotropy constant using both results in Figs. 2 and 4. For bias voltage varying from -300 to $+100$ mV, the $H_k(SL)$ can be deduced from hysteresis loops measured with $H_{//}$ fields (see Figs. 2(f)–2(h)). For bias larger than 100 mV, the soft layer has in-plane anisotropy and the hysteresis loops cannot be any more determined using $\Delta R(H_{\perp})$ curves as discussed before. We thus used the stars on $\Delta R_V(H_{\perp})$ curves to estimate H_k (see Figs. 4(c)–4(f)). For the last case, the error on the value is larger as indicated by the larger error bars in Fig. 5. The effective anisotropy energy per surface area K_s is plotted as a function of the bias voltage in Fig. 5. Two regimes are observed. From -300 mV to $+50$ mV, K_s stays constant, so the anisotropy is not affected by the voltage. Above $+50$ mV, a linear variation is observed and K_s switches from positive (out-of-plane anisotropy) to negative (in-plane anisotropy). Niranjana *et al.*¹⁵ found such a linear variation using *ab initio* calculations and propose to quantify it by calculating the slope β_s defined as $\Delta K_s = \beta_s E$, with $E = \Delta V / t_{MgO}$ the electric field and t_{MgO} the MgO layer thickness. The calculated slope is here equal to $\beta_s = -1150 \pm 50$ fJ $V^{-1} m^{-1}$.

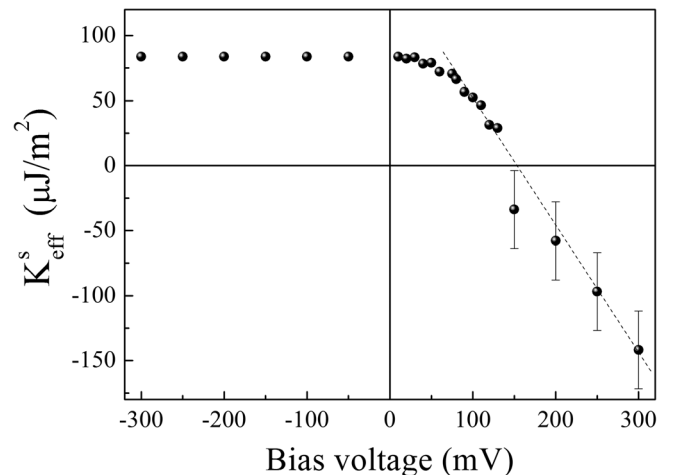


FIG. 5. Anisotropy K_s^{eff} as a function of the bias voltage applied to the MTJ. The dashed line is just a guide for the eye and has been used to determine the β parameter.

The effect of the electric field through the MgO barrier on the magnetic anisotropy is thus very strong here. Assuming first that the origin of this effect is charge variation at the Fe/MgO interface, electron depletion is inferred and calculated to be equal to 0.01 electrons per surface atom. This is larger than in previous reports^{8,12,17,19} and may explain why we manage to switch the magnetization from perpendicular to in-plane. Another point is the very large β_s value observed in this system, the largest reported up to now ($\beta_s = -1150 \pm 50 \text{ fJ V}^{-1} \text{ m}^{-1}$ here to compare to 50 in Ref. 9, 600 in Ref. 17, and 944 in Ref. 18). This is much larger than calculated values. Finally, the PMA is here suppressed by applying a positive ΔV which is contrary to results reported in Refs. 9, 12, and 18.

Thus far, several observations are not consistent with charge accumulation and depletion on an ideal capacitor. First, even so the SL anisotropy is quickly modified by the bias, the resistance of the MTJs is observed to slowly vary with time after biasing. Typical time transients are around several minutes to 1 h depending on the bias amplitude at room temperature, much larger than the delay time τ of charge accumulation or depletion in an ideal capacitor ($\tau = RC$ is close to 10^{-7} s for our samples where R is the circuit resistance and C the capacitance). Second, the variation of the soft layer anisotropy with the bias applied to the MgO dielectric layer is here observed only for positive bias, whereas symmetric effect may be observed regarding the very small charge accumulation at the interfaces (0.01 electron/atom). One possible explanation is that the MgO barrier does not behave like an ideal dielectric layer, due to defects in the MgO barrier, like vacancies or dislocations.²³ Thus, these defects may trap charges, and electromigration may occur to move these defects towards Fe/MgO interfaces as proposed in Ref. 18. Such trapping phenomenon may depend on the voltage polarity. The origin of this phenomenon may also come from the Fe/MgO interface. Bonell *et al.*²⁴ recently observed that using Fe/MgO interface with additional oxygen at the interface, the Fe-O hybridization is strongly affected by the electric field applied in the barrier. Finally, the last hypothesis is that the V/Fe interface plays a role. Indeed, we consider here that $K_{\text{shape}}(t - t_{DL})$ and the interface anisotropy at V/Fe interface do not depend on voltage. But so far, the mechanisms that may lead to such dependences at the V/Fe interface have to be evidenced.

In summary, epitaxial Fe(0.7 nm)/MgO/Fe(001) magnetic tunnel junctions were prepared such that the thin Fe electrode showed perpendicular magnetic anisotropy that is decreasing for a positive applied bias voltage through the MgO barrier. The electron depletion from the Fe(0.7 nm) / MgO interface is estimated around 0.01 electrons/atom at 300 mV, leading to a huge magnetic anisotropy variation with bias $\beta_s = -1150 \text{ fJ V}^{-1} \text{ m}^{-1}$. This is significantly larger

than calculated and experimental values reported up to now. Interestingly, negative bias has no influence on the MTJ anisotropy. The origin of the very high extracted values of β_s , the observed asymmetry, and the dependence on voltage polarity are not fully understood and will require further investigation.

We would like to thank Eric Fullerton for fruitful discussion, and Robert Tolley for improving the English of this paper. This work was supported by the French *Agence Nationale de la Recherche*, ELECMADÉ Project No. ANR-2010-BLANC-1006 and the Region Lorraine.

- ¹J. C. Slonczewski, *J. Magn. Magn. Mater.* **159**, L1 (1996).
- ²L. Berger, *J. Appl. Phys.* **55**, 1954 (1984).
- ³S. Mangin, Y. Henry, D. Ravelosoa, J. A. Katine, and E. E. Fullerton, *Appl. Phys. Lett.* **94**, 012502 (2009).
- ⁴V. Novosad, Y. Otani, A. Ohsawa, S. G. Kim, K. Fukamichi, J. Koike, K. Maruyama, O. Kitakami, and Y. Shimada, *J. Appl. Phys.* **87**, 6400 (2000).
- ⁵M. Overby, A. Chernyshov, L. P. Rokhinson, X. Liu, and J. K. Furdyna, *Appl. Phys. Lett.* **92**, 192501 (2008).
- ⁶H. Ohno, D. Chiba, F. Matsukura, T. Omiya, E. Abe, T. Dietl, Y. Ohno, and K. Ohtani, *Nature* **408**, 944 (2000).
- ⁷D. Chiba, M. Yamanouchi, F. Matsukura, and H. Ohno, *Science* **301**, 943 (2003).
- ⁸M. Weisheit, S. Fahler, A. Marty, Y. Souche, C. Poinsignon, and D. Givord, *Science* **315**, 349 (2007).
- ⁹T. Maruyama, Y. Shiota, T. Nozaki, K. Ohta, N. Toda, M. Mizuguchi, A. A. Tulapurka, T. Shinjo, M. Shiraishi, S. Mizukami, Y. Ando, and Y. Suzuki, *Nat. Nanotechnol.* **4**, 158 (2009).
- ¹⁰D. Chiba, S. Fukami, K. Shimamura, N. Ishiwata, K. Kobayashi, and T. Ono, *Nature Mater.* **10**, 853–856 (2011).
- ¹¹K. Shimamura, D. Chiba, S. Ono, S. Fukami, N. Ishiwata, M. Kawaguchi, K. Kobayashi, and T. Ono, *Appl. Phys. Lett.* **100**, 122402 (2012).
- ¹²Y. Shiota, S. Murakami, F. Bonell, T. Nozaki, T. Shinjo, and Y. Suzuki, *Appl. Phys. Express* **4**, 043005 (2011).
- ¹³C. G. Duan, J. P. Velez, R. F. Sabirianov, Z. Q. Zhu, J. H. Chu, S. S. Jaswal, and E. Y. Tsymlal, *Phys. Rev. Lett.* **101**, 137201 (2008).
- ¹⁴K. Nakamura, R. Shimabukuro, Y. Fujiwara, T. Akiyama, T. Ito, and A. J. Freeman, *Phys. Rev. Lett.* **102**, 187201 (2009).
- ¹⁵M. K. Niranjan, C.-G. Duan, S. S. Jaswal, and E. Y. Tsymlal, *Appl. Phys. Lett.* **96**, 222504 (2010).
- ¹⁶K. H. He, J. S. Chen, and Y. P. Feng, *Appl. Phys. Lett.* **99**, 072503 (2011).
- ¹⁷F. Bonell, S. Murakami, Y. Shiota, T. Nozaki, T. Shinjo, and Y. Suzuki, *Appl. Phys. Lett.* **98**, 232510 (2011).
- ¹⁸U. Bauer, M. Przybylski, J. Kirschner, and G. S. Beach, *Nano Lett.* **12**, 1437 (2012).
- ¹⁹T. Nozaki, Y. Shiota, M. Shiraishi, T. Shinjo, and Y. Suzuki, *Appl. Phys. Lett.* **96**, 022506 (2010).
- ²⁰M. Endo, S. Kanai, S. Ikeda, F. Matsukura, and H. Ohno, *Appl. Phys. Lett.* **96**, 212503 (2010).
- ²¹W.-G. Wang, M. E. Li, S. Hageman, and C. L. Chien, *Nature Mater.* **11**, 64 (2012).
- ²²C.-H. Lambert, A. Rajanikanth, T. Hauet, S. Mangin, E. Fullerton, and S. Andrieu, *Appl. Phys. Lett.* **102**, 122410 (2013).
- ²³F. Bonell, S. Andrieu, C. Tiusan, F. Montaigne, E. Snoeck, B. Belhadji, L. Calmels, F. Bertran, P. Le Fèvre, and A. Taleb-Ibrahimi, *Phys. Rev. B* **82**, 092405 (2010).
- ²⁴F. Bonell, Y. T. Takahashi, D. D. Lam, S. Yoshida, Y. Shiota, S. Miwa, T. Nakamura, and Y. Suzuki, *Appl. Phys. Lett.* **102**, 152401 (2013).